Transactions of JWRI, Vol. 37 (2008), No. 1

Behavior of Hydrogen in Super Duplex Stainless Steels†

KURODA Toshio* and NAKADE Katsuyuki**

Abstract

Hydrogen behavior in SAF2507 super duplex stainless steel and SAF2205 conventional duplex stainless steel was investigated by means of internal friction measurement. The internal friction measurements were conducted over a temperature range from 77K to 373K by using an inverted torsion pendulum for a frequency of 1.5Hz. A significant peak appeared at 245K after hydrogen charging of the super duplex stainless steel and conventional duplex stainless steel. The peak height increased with increasing hydrogen concentration. The peak was associated with hydrogen in austenite. As the specimens were heated at 1223K for various times, sigma phase consisting of Fe-Cr compound precipitated in the ferrite at the ferrite/austenite interface. The broadening of the internal friction peak at 245K and scattering of the internal friction value took place after hydrogen charging for the sigma phase precipitation. Overlapped two peaks of the peak associated with hydrogen in austenite and the peak associated with hydrogen in sigma phase were observed. The precipitation of sigma phase caused suppression of hydrogen diffusion in super duplex stainless steel. It is considered that hydrogen was dissolved in the sigma phase on the basis of the hydrogen measurement and internal friction measurement.

KEY WORDS: (Super duplex stainless steel) (Internal friction) (Hydrogen) (Austenite) (Snoek peak) (Sigma phase)

1. Introduction

Super duplex stainless steels consisting of a ferritic-austenitic mixed microstructure are superior in toughness, pitting corrosion resistance and stress corrosion cracking resistance and in addition, have an order of double the yield strength as compared with common austenitic stainless steels, and are thus being used extensively in the oil, gas, and petrochemical applications, particularly where chlorides are present [1)- 5)].

However, it has been reported that hydrogen embrittlement occurs in the ferrite phase at very low hydrogen concentrations [6)- 7)] in the duplex stainless steels. Furthermore, the precipitation of the sigma phase consisting of Fe-Cr compound occurs very quickly at temperatures between 923K and 1323K [1)- 5)]. Although two kinds of phenomenon will occur simultaneously in super duplex stainless steels, the effects of sigma phase on hydrogen behavior have not been reported. Consequently, it is important to clarify the effect of the sigma phase on hydrogen behavior.

The internal friction technique generally provides valuable information about hydrogen mobility and concentration in austenitic steels. Peterson et al [8)] first observed an internal friction peak of type 310 austenitic stainless steel containing hydrogen. Asano et al [9)] observed an internal friction peak located at about 300K for frequencies of 500Hz. This peak was interpreted in terms of the reorientation of paired hydrogen atoms in the applied stress field. Thus, internal friction effect due to hydrogen in fcc systems have been reviewed [9)- 11)], but the effect of sigma phase on hydrogen behavior in case of SAF2507 super duplex stainless steels has not been clarified[1)- 2)].

Therefore, the purpose of this research is to investigate the effect of sigma phase on hydrogen behavior in super duplex stainless steels by using internal friction measurements.

2. Experimental

The materials used in this investigation are SAF2507 super duplex stainless steel and SAF 2205 conventional duplex stainless steel with chemical compositions as shown in **Table 1**. The internal friction specimens were taken from each plate with 12 mm of thickness. Microstructure observation was performed

† Received on July 11, 2008
* Specially Appointed Professor
** Tokyo Electric Power Company, Inc.

Transactions of JWRI is published by Joining and Welding Research Institute, Osaka University, Ibaraki, Osaka 567-0047, Japan

Table 1 Chemical composition of SAF2507 super duplex stainless steel and SAF2205 conventional duplex stainless steel (mass%)

Grade	C	Si	Mn	P	S	Ni	Cr	Mo	N	Cu
SAF2205	0.018	0.44	0.90	0.018	0.001	5.91	22.77	3.25	0.14	—
SAF2507	0.014	0.30	0.91	0.017	0.0005	6.65	25.43	3.78	0.27	0.09

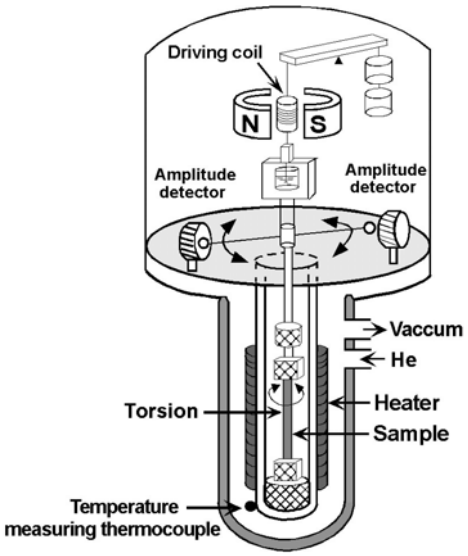

Fig.1 Schematic illustration of apparatus for internal friction measurement.

using electrolytic etching in 10 kmol/m^3 KOH solution. This etching technique colored sigma phase brown, colored ferrite blue and colored austenite white (in case of monochrome photographs, the etching technique colored sigma phase black, colored ferrite gray and colored austenite white).

The size of the internal friction specimen was 115.0 mm long, 4.8 mm wide and 0.8 mm thick. The internal friction specimens and X-ray specimens were cathodically charged at room temperature in a 5% sulphuric acid solution containing sodium arsenate as a catalytic agent promoting hydrogen entry. The current density was 200A/m^2. The measurement of total hydrogen content in the charged specimens was performed at 1973K by using a high sensitive hydrogen analyzer. The specimen size for this was the same as the internal friction specimen. X-ray diffraction with K_α radiation of copper target was employed to examine and confirm precipitation of sigma phase.

The internal friction measurement was conducted over a temperature range from 77K to 373K by using an inverted torsion pendulum at a frequency of about 1.5Hz. The schematic illustration of the internal friction

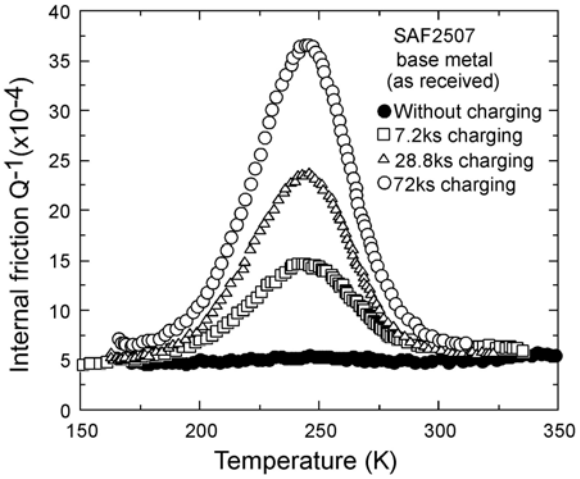

Fig. 2 Internal friction versus temperature curves of SAF2507 super duplex stainless steel.

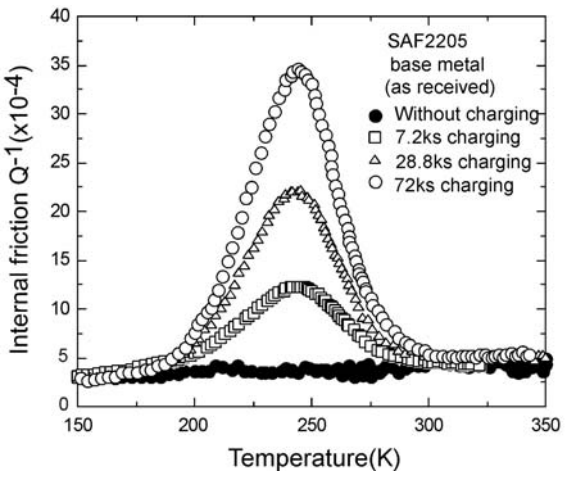

Fig.3 Internal friction versus temperature curves of SAF2205 conventional duplex stainless steel.

apparatus is shown in **Fig. 1**. The amplitude of free damping is A_0 in the early period and An in the nth cycle. The internal friction value Q^{-1} was calculated by the following equation.

$$Q^{-1} = [\,-1/(n\pi)]\ ln\ (A_n/A_0) \qquad (1)$$

3. Results and Discussion

Super duplex stainless steel has a microstructure consisting of elongated austenite along the rolling direction in the ferrite matrix. The volume fraction of the ferrite was approximately 65%, and the austenite was approximately 35%. Hydrogen can diffuse easily through the continuous ferrite when hydrogen charging is performed [12) - 13)]. The internal friction values (Q^{-1}) obtained for SAF2507 super duplex stainless steel were

plotted against absolute temperature in **Fig. 2**.

Without hydrogen charging, an internal friction peak was hardly observed. The internal friction peak appeared at 245K after hydrogen charging.The peak height increased with increasing hydrogen charging time. The symmetrical peak is considered to be due to hydrogen in the austenite.

The temperature range of internal friction curves plotted was between 150K and 350K, because no peak was observed below 150K. In the as-received condition without hydrogen-charging, no peak was present. It is considered that hydrogen diffuses to the ferrite and diffuses to the austenite as a result hydrogen charging. Therefore, the sigma phase precipitated in the ferrite suppresses the fast hydrogen diffusion.

Gibara et al [8] found the hydrogen Snoek peak occurred at 48K at 80kHz in bcc iron containing hydrogen, furthermore Gibara et al [10] and Asano et al [11] reported that there was a cold-work peak caused by hydrogen-dislocation interaction in cold-worked ferrite steel over the temperature range from 77K to room temperature. However a Snoek peak due to hydrogen in ferrite was not observed above 77K in this research, and a cold worked peak did not occur because the specimens were not cold-worked. Therefore, it was concluded that this observed peak was due to hydrogen in the austenite of the duplex stainless steel. The peak height increased as the hydrogen charging time increased up to 72ks.

Figure 3 shows internal friction versus temperature curves of SAF2205 conventional duplex stainless steel. No internal friction peak was observed without hydrogen charging. By hydrogen charging, a peak due to hydrogen was also found at 245K similar to SAF2507 super duplex stainless steel shown in Fig.2. The peak height increased as the hydrogen charging time increased up to 72ks. According to the microstructure observation, the volume fraction of ferrite was approximately 55%, and austenite was approximately 45%.

Figure 4 indicates internal friction curves of SAF2507 super duplex stainless steel reheated at 1223 K for 1.8 ks. After the same time charging, the peak height was decreased as compared to the as-received specimen in Fig.2. For the charging time of 72ks, the peak height Q^{-1} for hydrogen in as-received specimen is 37×10^{-4} as shown in Fig. 2, otherwise in case of the reheated specimen, as shown in Fig.4, the peak height Q^{-1} is 18×10^{-4}. Consequently, it can be concluded that hydrogen concentration in the austenite is much lower in the specimen containing sigma phase. The beginning of sigma phase precipitation was observed at ferrite/ widmanstätten primary austenite boundaries, and then the sigma phase continuously precipitated and the ferrite almost decomposed the sigma phase and the secondary austenite after reheating at 1223 K for 1.8 ks. The low peak height has been attributed to the reduction of hydrogen concentration in the austenite owing to the precipitation of the sigma phase and the secondary austenite.

T. Kuroda et al [12) 13)] reported that the peak height was mainly affected by hydrogen concentration (H_γ) and volume fraction of austenite (V_γ). Peak height $Q^{-1}{}_\gamma = V_\gamma \times H_\gamma$,but the volume fraction of austenite hardly changed after reheating at 1023K for 72ks, therefore the lowering of peak height is mainly due to the decrease of hydrogen concentration in austenite. The broadening of the peak and scattering of the internal friction value occurred as a result of sigma phase precipitation. This suggests that hydrogen-sigma phase interaction may be occurring, and it implies hydrogen present in the sigma phase lattice or trapped hydrogen or trapped molecular hydrogen at sigma/austenite interfaces.

Figure 5 shows the internal friction curves of

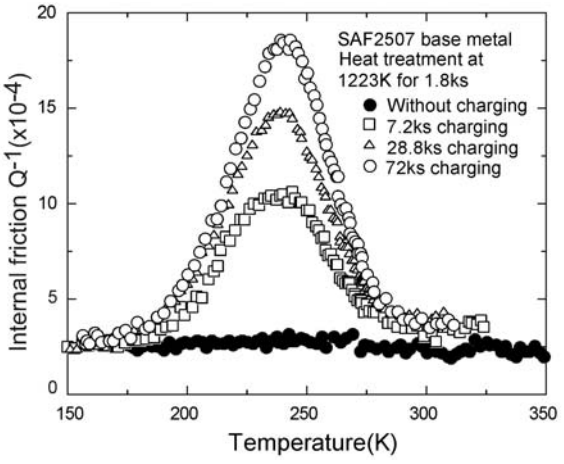

Fig. 4 Internal friction curves of reheated SAF2507 super duplex stainless steel.

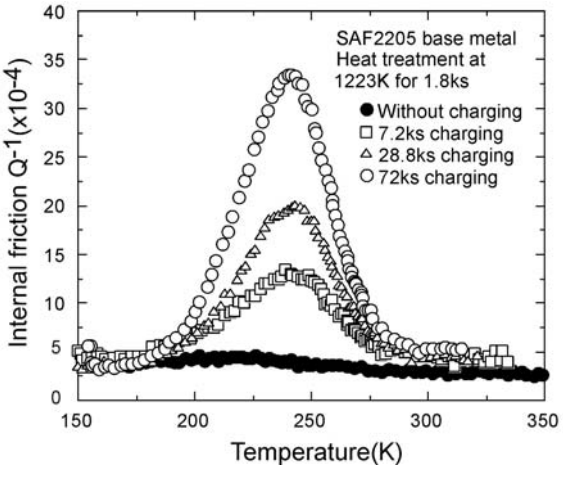

Fig.5 Internal friction curves of reheated SAF2205 super duplex stainless steel.

SAF2205 duplex stainless steel reheated at 1223 K for 1.8 ks. After hydrogen charging, the peak height was substantially lower than that of as-received specimen shown in Fig.3. This has been attributed to the reduction of hydrogen concentration in the austenite owing to the precipitation of the sigma phase. This would be supported if total hydrogen concentration was substantially smaller in the material with precipitated sigma phase, in which the ferrite decomposition caused a lower ability of hydrogen diffusion inside of the sample. If this peak is only due to hydrogen in austenite, it should show an internal friction spectrum with single relaxation time, as a symmetric curve with respect to the peak position.

However the sigma phase precipitation caused not only suppression of the internal friction peak height but also the broadening the peak at 245K and scattering of the internal friction value. Since the phenomenon occurred in the duplex stainless steel weld metal containing sigma phase, another internal friction peak due to hydrogen-sigma phase interaction may occur at lower temperatures than 245K as shown in **Fig.6**.

This implies a small amount of hydrogen exists in the sigma phase lattice or as trapped hydrogen at sigma/austenite phase boundaries. This means trapped hydrogen at the interfaces of sigma/austenite, and the hydrogen atom (H) at sigma/austenite phase boundaries implies weakly trapped hydrogen at the interfaces of sigma/austenite.

The internal friction peak height due to hydrogen in austenite was significant higher in as-received super duplex stainless steel, because the diffusivity of hydrogen in ferrite was much faster.

Figure 7 shows the proposed mechanism of an internal friction peak in fcc crystal. Hydrogen is located in the tetrahedral sites of A,B and C. Vacancy radius in an octahedral site is 5.3 nm and the radius of a hydrogen atom is 4.6 nm. A pair of hydrogens will give rise to Snoek relaxation peak of internal friction. Hydrogen damping occurs from site A to site B. An elastic behavior doed not appear. However a pair of hydrogen atoms moves from site A to site B. The anelastic behavior occurrs.The lower peak height indicates hydrogen diffusivity in sigma phase or sigma/austenite phase boundaries is substantially lower than that in the ferrite.

The sigma phase[14)-16)] has several tetrahedral interstitial sites**.**

Figure 8 shows the schematic illustration of hydrogen existence in the crystal of sigma phase. It is assumed that the hydrogen atom can enter into sigma phase structure if the space of the interstitial sites is bigger than that of hydrogen atom. Discussion of only two sites was performed here although there are four tetrahedral sites in lattice of sigma phase. If the hydrogen atom enters into a tetrahedral G1 site (0.04nm in radius), four neighbor substitution atoms (A1,B1,B2 and A2) will distort symmetry by 0.006nm. Hydrogen atoms can enter with strained 0.002nm in case of tetrahedral G2 site. This strain is the same phenomena as the moment of the

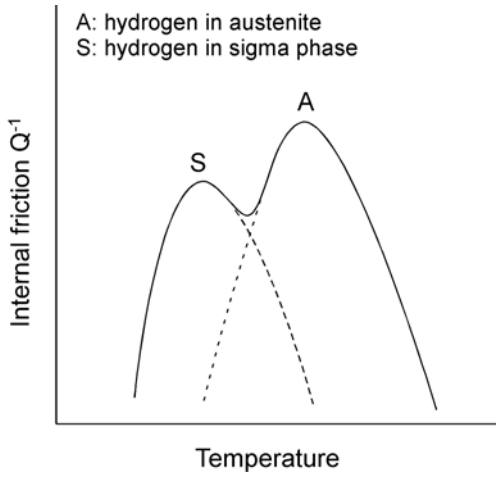

Fig.6 Schematic illustration of separation of two peaks

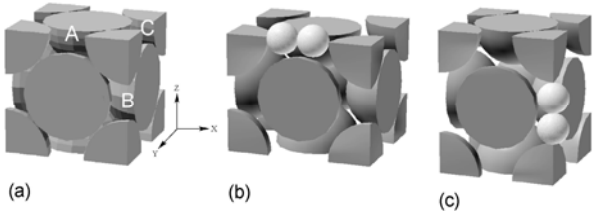

Fig.7 An interstitial-interstitial pair mechanism for a unit cell of face centered cubic.(fcc) lattice.

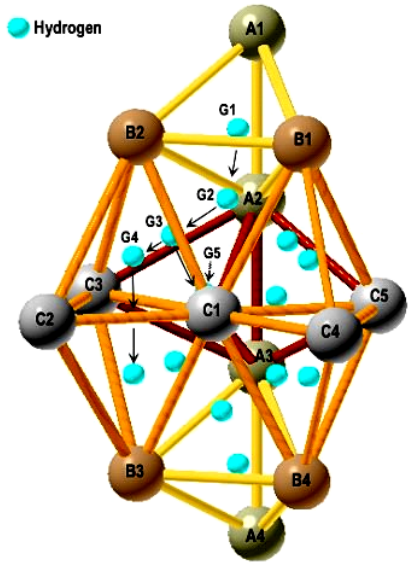

Fig.8 Schematic illustration of hydrogen in the crystal sigma phase lattice.

tetrahedral G1site.

However hydrogen must cross a saddle point before the hydrogen atom present in the tetrahedral G1 site can move to the tetrahedral G2 site. The diffusion of hydrogen atom will not take place easily, because hydrogen must distort three neighboring substitution atoms (A2, B1 and B2) when the hydrogen atom crosses the saddle point. The passing point is the medium point of triangle B1, B2 and A2. It is assumed that it is impossible to locate hydrogen in these interstitial sites because the size of interstitial sites is a little smaller than that of hydrogen atom, and consequently implies that the solubility of hydrogen in sigma phase is substantially smaller than that of an fcc crystal by geometrical considerations.

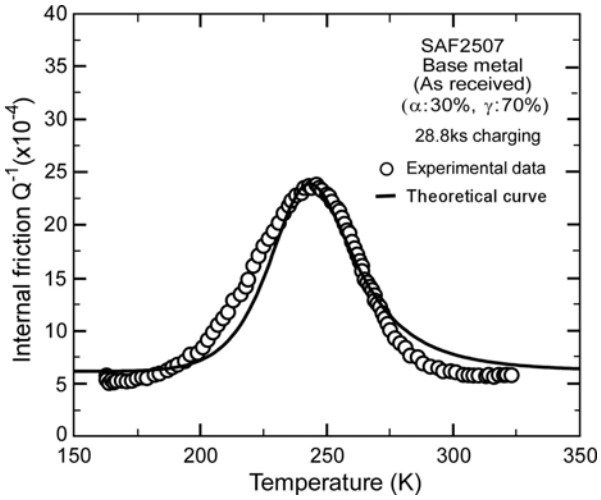

Fig.9 Comparison of experimental data and theoretical calculation for the internal friction curve after hydrogen charging in SAF2507 super duplex stainless steel.

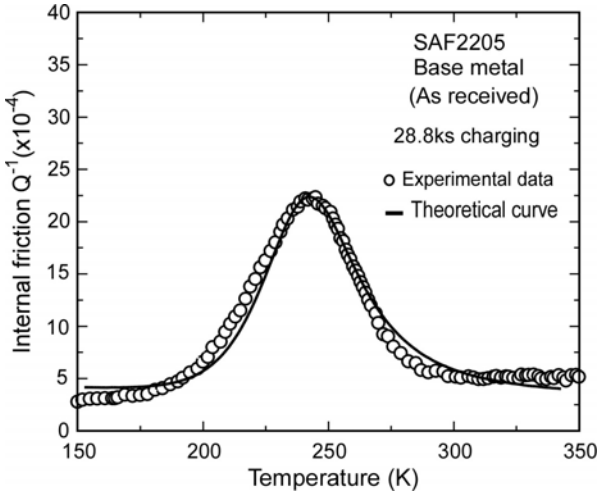

Fig.10 Comparison of experimental data and theoretical calculation for the internal friction curve after hydrogen charging in SAF2205 conventional duplex stainless steel.

Figure 9 indicates the internal friction versus temperature curves of SAF2507 super duplex stainless steel with experimental data and a theoretical curve. An activation energy of hydrogen diffusion in austenite was measured for super duplex stainless steels. A Snoek relaxation peak is generally observed in bcc materials. The internal friction value Q^{-1} is theoretically described. as follows.

$$Q^{-1} = sec\ [\ H / R\ (1 / T - 1 / T_p)\ ] \qquad (2)$$

H is activation energy, Tp is peak temperature and R is the gas constant. Experimental data are described as open circles. The calculated curve is shown as a solid line. The activation energy of hydrogen is calculated from the half width of the peak. Hγ is 33.0 kJ/mol. The result obtained in the present research is smaller than another report which recorded 52 kJ/mol.

Figure 10 shows the internal friction versus temperature curves of SAF2205 conventional duplex stainless steel with experimental data and the theoretical curve. An activation energy of hydrogen diffusion in austenite was measured for duplex stainless steels using Eq.(2). The activation energy was also 33.0 kJ/mol.

Figure 11 indicates the internal friction curves of the sigma phase precipitation samples with experimental data and theoretical curves for SAF2507 super duplex stainless steel. Peak spectra show both a symmetry and broadening. This is considered to be an overlapping of

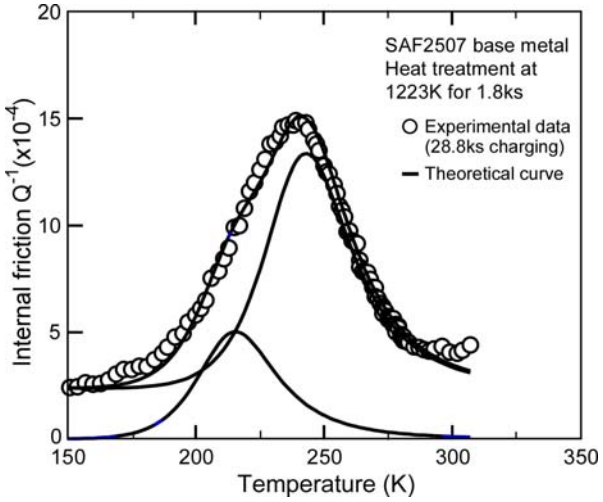

Fig.11 Comparison of experimental data and theoretical calculation for the internal friction curve after hydrogen charging in reheated SAF2507 super duplex stainless steel.

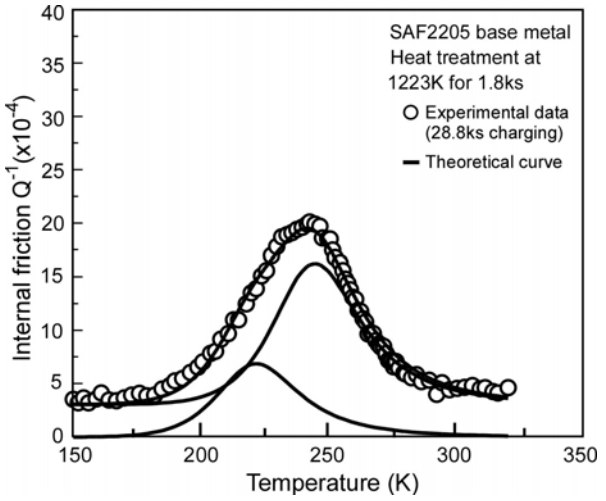

Fig.12 Comparison of experimental data and theoretical calculation for the internal friction curve after hydrogen charging in reheated SAF2205 conventional duplex stainless steel.

two peaks. In case of as-received samples, only one spectrum was observed at 245 K for hydrogen in austenite. However, two peaks are observed for the specimens consisting austenite and sigma phase. The activation energy of hydrogen in the sigma phase was evaluated as 28.4 kJ/mol, using mathematical analysis.

Figure 12 indicates the internal friction curves of the sigma phase precipitation samples with experimental data and theoretical curves for SAF2205 conventional duplex stainless steel, two calculation curves were evaluated representing hydrogen in austenite and hydrogen in sigma phase. As a result, the activation energy of hydrogen diffusion in sigma phase was found to be 25kJ/mol at 220K.

4. Conclusions

Hydrogen behavior in SAF2507 super duplex stainless steel and SAF2205 conventional duplex stainless steel was investigated by means of internal friction measurements. The internal friction measurements were conducted over the temperature range from 77K to 373K using an inverted torsion pendulum at a frequency of1.5Hz.

(1)A significant peak appeared at 245K after hydrogen charging for both super duplex stainless steel and conventional duplex stainless steel. The peak height increased with increasing hydrogen concentration. The peak was associated with hydrogen in austenite.

(2)As the specimens were heated at 1223 K for 1.8 ks, sigma phase precipitated in the ferrite at the ferrite/austenite interface. The broadening of the internal friction peak at 245 K and scattering of the internal friction value took place by hydrogen charging for the sigma phase precipitation. The overlapping of two peaks, that associated with hydrogen in austenite and that associated with hydrogen in sigma phase was observed.

(3)The precipitation of sigma phase caused suppression of hydrogen diffusion in duplex stainless steel and weld metal. It is considered that hydrogen was dissolved in the sigma phase on the basis of the hydrogen content measurement and internal friction measurement.

(4)According to geometric calculations of the crystal structure of sigma phase, hydrogen atoms easily move into tetragonal sites of the sigma phase lattice.

Acknowledgement

This work was supported by Grant-in-Aid for Cooperative Research Project of Nationwide Joint-Use Research Institute on Development Base of Joining Technology for New Metallic Glasses and Inorganic Materials from The Ministry of Education, Culture, Sports, Science and Technology, Japan.

References

1) T.Kuroda, K. Nakade and K. Ikeuchi, Welding in the world, 44, (2000) 17-22.
2) T.kuroda, K.Ikeuchi, K.Oe, K.Nakade, Proceedings Materials Solutions Conference ’99 on Joining of Advanced and Specialty Materials, 1-4 November 1999, Ohio.
3) J.O.Nilsson, Mater.Sci.and Tech.,8, (1992) 685-699.
4) O.Nilsson and A.Wilson, Mater.Sci.and Tech., 9 545 (1993).
5) R.A.Walker, Mater.Sci.and Tech., 4,78-84 (1988).
6) D.J.Kotecki, Welding Journal, 10 (1986) 273s.
7) T.Kuroda and C.D.Lundin, Journal of Society Material Science Japan, 43 (1994) 562.
8) J. A. Peterson, R. Gibala, and A.R. Troiano, Journal of The Iron and Steel Institute (1969), 86.
9) H.Asano, K. Sumida and M.Otsuka, J. Japan Inst. Metals, 41 (1985) 671.
10) R.Gibala., Transaction of the Metallurgical society of AIME, 239 (1967) 1574.
11) M.Kazaoka and H.Asano, J.Japan Inst.Metals, 50 (1986) 391.
12) T.Kuroda, Y.Kikuchi and A.Kasahara, Materials Sci. Research international, 4-3, (1998) 217-222.
13) T.Kuroda, A.Kasahara, K.Nakade; Quatt. J. Japan Welding Society, v 45, n 11 (1999) p 45.
14) G.Bergman and D.P.Shoemaker, Acta Cryst. 7, (1954), 857.
15) J.S. Kasper and R.M.Waterstrat, Acta Cryst. 9, (1956), 289.
16) G.J.Dickins, A,Audrey, M.B.Douglas and W.H.Taylor, Acta. Cryst., 9, (1956), 297.
17) T.Kuroda, Trans. JWRI, 26-2, (2007), 61-66.